

NLO QCD corrections to B_c -pair production in photon-photon collision

Zi-Qiang Chen^{1†}, Hao Yang^{1‡} and Cong-Feng Qiao^{1,2*}

¹ *School of Physics, University of Chinese Academy of Science,*

Yuquan Road 19A, Beijing 10049

² *CAS Key Laboratory of Vacuum Physics, Beijing 100049, China*

Abstract

The B_c meson pair, including pairs of both pseudoscalar states and vector states, productions in high energy photon-photon interaction are investigated at the next-to-leading order (NLO) accuracy in the nonrelativistic quantum chromodynamics (NRQCD) factorization formalism. The corresponding cross sections at the future e^+e^- colliders with $\sqrt{s} = 250$ GeV and 500 GeV are evaluated. Numerical result indicates that the inclusion of the NLO corrections shall greatly suppress the scale dependence and enhance the prediction reliability. In addition to the phenomenological meaning, the NLO QCD calculation of this process subjects to certain technical issues, which are elucidated in details and might be applicable to other relevant investigations.

PACS numbers: 12.38.Bx, 12.39.Jh, 14.40.Pq, 14.70.Bh

[†] chenziqiang13@mails.ucas.ac.cn

[‡] yanghao174@mails.ucas.ac.cn

* qiaocf@ucas.ac.cn, corresponding author

I. INTRODUCTION

As the only heavy meson consisting of two heavy quarks with different flavors, the B_c meson is of great interest in both experiment and theory. Study of its production and decays may enrich our knowledge on the properties of double heavy meson and the nature of perturbative QCD (pQCD). The ground state of B_c meson, $B_c^+(1S)$, was discovered by CDF Collaboration [1, 2] in 1998. And its excited state $B_c^+(2S)$ was observed by ATLAS [3] and CMS [4] Collaboration in 2014 and 2019 respectively.

Due to the large mass of bottom and charm quarks, the production of heavy quark pair can be described by pQCD, while the hadronization process can be factored by using the NRQCD factorization formalism [5]. For inclusive B_c meson production, various investigations have been carried out, including the direct production through pp [6–9], e^+e^- [10, 11], $\gamma\gamma$ [12, 13] and ep [14, 15] collisions, and the indirect production through top quark [16, 17], Z boson [18–21], W boson [22–24] and Higgs boson [25] decays.

In processes of QCD and quantum electromagnetic dynamics (QED), the B_c^+ meson is produced in accompany with one additional $b\bar{c}$ pair. Hence there are certain probabilities for $b\bar{c}$ to form another $b\bar{c}$ meson, namely the B_c -pair exclusive production. Generally speaking, the experiment measurement of exclusive process possesses a relative high precision, which is required in exploring the properties of QCD and hadrons. In the literature, various B_c -pair production processes have been investigated, including in pp [26, 27], e^+e^- [28–30] and $\gamma\gamma$ [26] collisions. We notice that in Ref.[26] the leading order (LO) analysis on B_c -pair production in photon-photon collision was performed, however with only $B_c^+ + B_c^-$ (pseudoscalar-pseudoscalar, PP) and $B_c^{*+} + B_c^{*-}$ (vector-vector, VV) configurations being considered. In this work, for the sake of completeness we first repeat the LO calculation in [26] and then calculate the LO B_c -pair production in $B_c^+ + B_c^{*-}$ (pseudoscalar-vector, PV) and $B_c^{*+} + B_c^-$ (vector-pseudoscalar, VP) configurations¹. In the end, all these processes will be evaluated up to the NLO

¹ The PV and VP production are related by a charge-conjugation transformation. Their cross section

QCD accuracy. Note, hereafter for simplicity the B_c represents for both pseudoscalar B_c and vector B_c^* , which may overwhelmingly decay to the pseudoscalar state, unless specifically mentioned.

The rest of the paper is organized as follows. In section II we present the primary formulae employed in the calculation. In section III, some technical details in the analytical calculation are given. In section IV, the numerical evaluation for concerned processes is performed. The last section is remained for summary.

II. FORMULATION

According to NRQCD factorization formalism, the cross section of B_c -pair production via photon-photon fusion can be formulated as

$$d\hat{\sigma}(\gamma + \gamma \rightarrow B_c^+ + B_c^-) = \frac{|\psi(0)|^4}{2\hat{s}} \frac{1}{4} \sum |\mathcal{M}(\gamma + \gamma \rightarrow [c\bar{b}] + [b\bar{c}])|^2 d\text{PS}_2, \quad (1)$$

where $\psi(0)$ is the wave function of B_c meson at the origin, \hat{s} is the center-of-mass energy square for the two photons, \sum sums over the polarizations and colors of the initial and final particles, $\frac{1}{4}$ comes from the spin average of the initial $\gamma\gamma$ states, $\mathcal{M}(\gamma + \gamma \rightarrow [c\bar{b}] + [b\bar{c}])$ is the corresponding partonic amplitude, $d\text{PS}_2$ stands for the two-body phase space.

The partonic amplitude can be computed by using the covariant projection operator method. At the leading order of the relative velocity expansion, it is legitimate to take $m_{B_c} = m_b + m_c$, $p_{B_c} = p_c + p_b = (1 + \frac{m_c}{m_b})p_b$. The spin and color projection operator has the form

$$\Pi(n) = \frac{1}{2\sqrt{m_{B_c}}} \epsilon^{(n)} (\not{p}_{B_c} + m_{B_c}) \otimes \left(\frac{1_c}{\sqrt{N_c}} \right), \quad (2)$$

where $\epsilon(^1S_0) = \gamma_5$, $\epsilon(^3S_1) = \not{\epsilon}$ and ϵ is the spin polarization for B_c^* meson. The 1_c stands for the unit color matrix, and $N_c = 3$ for the number of colors in QCD.

The photon-photon scattering can be achieved in high energy e^+e^- collider like the

are exactly the same.

Large Electro-Positron Collider (LEP), the Circular Electron Positron Collider (CEPC) and the International Linear Collider (ILC), or in hadron collider like the Large Hadron Collider (LHC). Here we focus only on the e^+e^- collision case, where the initial photon can be generated by the bremsstrahlung or by the laser back scattering (LBS) effect. The cross section are then formulated as

$$d\sigma(e^+ + e^- \rightarrow e^+ + e^- + B_c^+ + B_c^-) = \int dx_1 dx_2 f_\gamma(x_1) f_\gamma(x_2) d\sigma(\gamma + \gamma \rightarrow B_c^+ + B_c^-), \quad (3)$$

where $f_\gamma(x)$ is the photon distribution with the fraction x of the beam energy.

Imposing transverse momentum cut $p_T^- < p_T < p_T^+$ and rapidity cut $|y| < y_c$ to each B_c meson, the formula for total cross section is

$$\begin{aligned} & \sigma(e^+ + e^- \rightarrow e^+ + e^- + B_c^+ + B_c^-) \\ &= \frac{1}{256\pi} \left\{ \theta(y_c - \ln \frac{2m_T^-}{\sqrt{s}}) \int_{\ln \frac{2m_T^-}{\sqrt{s}}}^{\ln \frac{2m_T^+}{\sqrt{s}}} dX \int_{\max\{-y_T^+, -y_c\}}^{\min\{y_T^+, y_c\}} dy^* \frac{\text{sech}^2 y^*}{E_1^2} \sum |\mathcal{M}|^2 \right. \\ & \quad \int_{\max\{-y_c + y^*, X\}}^{\min\{y_c - y^*, -X\}} dy_0 x_1 f_\gamma(x_1) x_2 f_\gamma(x_2) + \theta(y_c - \ln \frac{2m_T^+}{\sqrt{s}}) \int_{\ln \frac{2m_T^+}{\sqrt{s}}}^{\min\{0, \ln(\frac{2m_T^+}{\sqrt{s}} \cosh y_c)\}} dX \\ & \quad \left(\int_{y_T^-}^{\min\{y_T^+, y_c\}} dy^* + \int_{\max\{-y_T^+, -y_c\}}^{-y_T^-} dy^* \right) \frac{\text{sech}^2 y^*}{E_1^2} \sum |\mathcal{M}|^2 \\ & \quad \left. \int_{\max\{-y_c + y^*, X\}}^{\min\{y_c - y^*, -X\}} dy_0 x_1 f_\gamma(x_1) x_2 f_\gamma(x_2) \right\}, \end{aligned} \quad (4)$$

with

$$\begin{aligned} X &= \frac{1}{2} \ln(x_1 x_2), \quad y_0 = \frac{1}{2} \ln \frac{x_1}{x_2}, \\ m_T^\pm &= \sqrt{m_{B_c}^2 + p_T^\pm}, \\ y_T^\pm &= \frac{1}{2} \ln \frac{E_1 + \sqrt{E_1^2 - m_T^{\mp 2}}}{E_1 - \sqrt{E_1^2 - m_T^{\mp 2}}}. \end{aligned} \quad (5)$$

Here, \sqrt{s} is the collision energy for e^+e^- collider, $E_1 = \sqrt{s x_1 x_2}/2$ and $y^* = y - y_0$ are the energy and rapidity of B_c meson in the photon-photon center-of-mass system, $\theta(x)$ means the unit step function.

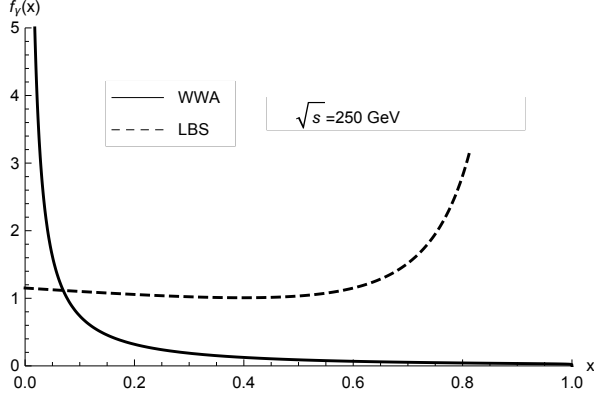


FIG. 1: The spectra of WWA photon and LBS photon at $\sqrt{s} = 250$ GeV.

The spectrum of bremsstrahlung photon can be well formulated in the Weizsacker-Williams approximation (WWA) as [31]

$$f_{\gamma}(x) = \frac{\alpha}{2\pi} \left[\frac{1 + (1-x)^2}{x} \log \left(\frac{Q_{\max}^2}{Q_{\min}^2} \right) + 2m_e^2 x \left(\frac{1}{Q_{\max}^2} - \frac{1}{Q_{\min}^2} \right) \right], \quad (6)$$

where $Q_{\min}^2 = m_e^2 x^2 / (1-x)$ and $Q_{\max}^2 = Q_{\min}^2 + (\theta_c \sqrt{s} / 2)^2 (1-x)$ with $x = E_{\gamma} / E_e$, θ_c is the experimental angular cut which taken to be 32 mrad here. For the LBS photon, the spectrum is expressed as [32]

$$f_{\gamma}(x) = \frac{1}{N} \left[1 - x + \frac{1}{1-x} - 4r(1-r) \right], \quad (7)$$

where $r = \frac{x}{x_m(1-x)}$ and the normalization factor

$$N = \left(1 - \frac{4}{x_m} - \frac{8}{x_m^2} \right) \log(1+x_m) + \frac{1}{2} + \frac{8}{x_m} - \frac{1}{2(1+x_m)^2}. \quad (8)$$

Here $x_m \simeq 4.83$ [33] and the energy fraction x of photon is restricted in $0 \leq x \leq x_m / (1+x_m)$. The behaviors of WWA photon and LBS photon are quite different, their spectra at $\sqrt{s} = 250$ GeV are shown in Fig.1.

III. ANALYTICAL CALCULATION

The typical tree-level and one-loop Feynman diagrams for the partonic process are shown in Fig.2. The momenta and the polarization vectors for the incoming and

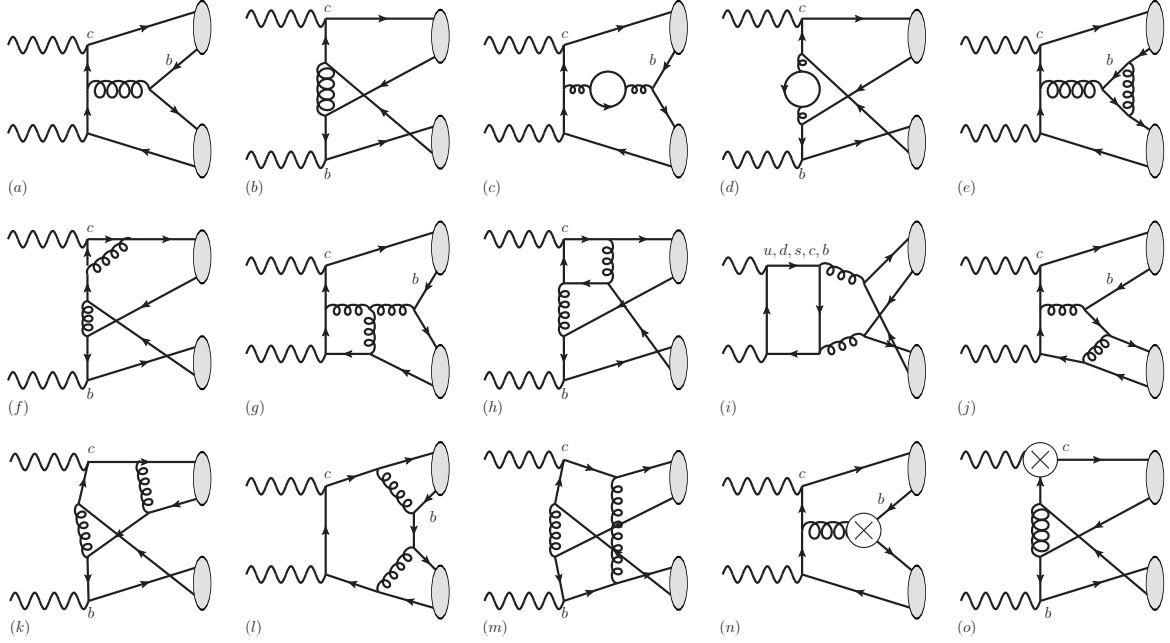


FIG. 2: Typical tree-level and one-loop Feynman diagrams for the partonic process (9).

outgoing particles are denoted as:

$$\gamma(p_1, \epsilon_1) + \gamma(p_2, \epsilon_2) \rightarrow [\bar{c}b](k_1, \epsilon_3) + [\bar{c}b](k_2, \epsilon_4). \quad (9)$$

All initial and final state particles are on the mass shell: $p_1^2 = p_2^2 = 0$ and $k_1^2 = k_2^2 = m_{B_c}^2$. The polarization vectors satisfy the constraint: $\epsilon_1 \cdot \epsilon_1^* = \epsilon_2 \cdot \epsilon_2^* = \epsilon_3 \cdot \epsilon_3^* = \epsilon_4 \cdot \epsilon_4^* = -1$ and $p_1 \cdot \epsilon_1 = p_2 \cdot \epsilon_2 = k_1 \cdot \epsilon_3 = k_2 \cdot \epsilon_4 = 0$.

To proceed the calculation, we notice working in the photon-photon center-of-mass system is convenient. By introducing the orthonormal four-vector base: $n_0 = (1, 0, 0, 0)$, $n_1 = (0, 1, 0, 0)$, $n_2 = (0, 0, 1, 0)$ and $n_3 = (0, 0, 0, 1)$, we may choose

$$\begin{aligned} p_1 &= E_1(n_0 + n_3), & p_2 &= E_1(n_0 - n_3), \\ k_1 &= E_1(n_0 + r_y n_2 + r_z n_3), & k_2 &= E_1(n_0 - r_y n_2 - r_z n_3). \end{aligned} \quad (10)$$

and

$$\epsilon_1^{(1)} = n_1, \quad \epsilon_1^{(2)} = n_2, \quad \epsilon_2^{(1)} = n_1, \quad \epsilon_2^{(2)} = n_2;$$

$$\begin{aligned}
\epsilon_3^{(1)} &= n_1, \quad \epsilon_3^{(2)} = \frac{r_z n_2 - r_y n_3}{\sqrt{r_y^2 + r_z^2}}, \quad \epsilon_3^{(3)} = \frac{(r_y^2 + r_z^2)n_0 + r_y n_2 + r_z n_3}{r_m \sqrt{r_y^2 + r_z^2}}; \\
\epsilon_4^{(1)} &= n_1, \quad \epsilon_4^{(2)} = \frac{r_z n_2 - r_y n_3}{\sqrt{r_y^2 + r_z^2}}, \quad \epsilon_4^{(3)} = \frac{(r_y^2 + r_z^2)n_0 - r_y n_2 - r_z n_3}{r_m \sqrt{r_y^2 + r_z^2}}.
\end{aligned} \tag{11}$$

Here $E_1 = \sqrt{s x_1 x_2}/2$, $r_y = k_y/E_1$, $r_z = k_z/E_1$, $r_m = m_{B_c}/E_1$, and the on shell condition constrain $r_y^2 + r_z^2 + r_m^2 = 1$. Then, the helicity amplitudes can be calculated straightforwardly through

$$\begin{aligned}
\mathcal{M}_{\text{PP}}^{ij} &= A_{\text{PP}}^{\mu\nu} \epsilon_{1\mu}^{(i)} \epsilon_{2\nu}^{(j)}, \\
\mathcal{M}_{\text{PV}}^{ijk} &= A_{\text{PV}}^{\mu\nu\rho} \epsilon_{1\mu}^{(i)} \epsilon_{2\nu}^{(j)} \epsilon_{3\rho}^{(k)}, \\
\mathcal{M}_{\text{VP}}^{ijk} &= A_{\text{VP}}^{\mu\nu\rho} \epsilon_{1\mu}^{(i)} \epsilon_{2\nu}^{(j)} \epsilon_{4\rho}^{(k)}, \\
\mathcal{M}_{\text{VV}}^{ijkl} &= A_{\text{VV}}^{\mu\nu\rho\sigma} \epsilon_{1\mu}^{(i)} \epsilon_{2\nu}^{(j)} \epsilon_{3\rho}^{(k)} \epsilon_{4\sigma}^{(l)}.
\end{aligned} \tag{12}$$

The tree-level calculation is straightforward, however the full analytic expressions of helicity amplitudes are still too lengthy to present in the mainbody of text. Considering of the symmetry property in amplitudes, we give the LO results in Appendix.

In the computation of one-loop amplitudes, the conventional dimensional regularization with $D = 4 - 2\epsilon$ is adopted to regularize the ultraviolet (UV) and infrared (IR) singularities. The IR singularities are canceled each other and the UV singularities are removed by renormalization procedure. The renormalization constants include Z_2 , Z_m , Z_3 and Z_g , which corresponding to heavy quark field, heavy quark mass, gluon field and strong coupling constant, respectively. We define Z_2 and Z_m in the on-shell (OS) scheme, Z_3 and Z_g in the modified minimal-subtraction ($\overline{\text{MS}}$) scheme. The corresponding counterterms are

$$\begin{aligned}
\delta Z_2^{\text{OS}} &= -C_F \frac{\alpha_s}{4\pi} \left[\frac{1}{\epsilon_{\text{UV}}} + \frac{2}{\epsilon_{\text{IR}}} - 3\gamma_E + 3 \ln \frac{4\pi\mu^2}{m^2} + 4 \right], \\
\delta Z_m^{\text{OS}} &= -3C_F \frac{\alpha_s}{4\pi} \left[\frac{1}{\epsilon_{\text{UV}}} - \gamma_E + \ln \frac{4\pi\mu^2}{m^2} + \frac{4}{3} \right], \\
\delta Z_3^{\overline{\text{MS}}} &= \frac{\alpha_s}{4\pi} (\beta_0 - 2C_A) \left[\frac{1}{\epsilon_{\text{UV}}} - \gamma_E + \ln(4\pi) \right], \\
\delta Z_g^{\overline{\text{MS}}} &= -\frac{\beta_0}{2} \frac{\alpha_s}{4\pi} \left[\frac{1}{\epsilon_{\text{UV}}} - \gamma_E + \ln(4\pi) \right].
\end{aligned} \tag{13}$$

Here, μ is the renormalization scale, γ_E is the Euler's constant; the mass m stands for m_c and m_b accordingly; $\beta_0 = (11/3)C_A - (4/3)T_F n_f$ is the one-loop coefficient of QCD beta function, n_f is the number of active quarks which taken to be 5 in our calculation; $C_A = 3$, $C_F = 4/3$ and $T_F = 1/2$ are color factors. Note, in the final results, all the δZ_3 terms are cancelled with each other.

We provide the analytic results for one-loop amplitudes as supplementary files attached to the arXiv preprint. In the NLO calculation, the Mathematica package FeynArts [34] is used to generate Feynman diagrams and Feynman amplitudes; FeynCalc [35, 36] and FORM [37, 38] are used to perform algebraic calculation; The package FIRE [39, 40] is employed to reduce the Feynman integrals into typical master integrals A_0 , B_0 , C_0 and D_0 , which are numerically evaluated by LoopTools [41].

IV. NUMERICAL RESULTS

In the numerical analysis, the formula (4) is used, with $|\mathcal{M}|^2 \simeq |\mathcal{M}_{\text{tree}}|^2$ for the LO calculation and $|\mathcal{M}|^2 \simeq |\mathcal{M}_{\text{tree}}|^2 + 2\text{Re}(\mathcal{M}_{\text{loop}}\mathcal{M}_{\text{tree}}^*)$ for the NLO calculation. The rapidity and p_T cuts, $|y| < 2$ and $2 < p_T < 40$ GeV, are imposed to each B_c meson. Other parameters used in numerical evaluation go as follows:

$$\begin{aligned} \alpha &= 1/137.065, \quad m_e = 0.511 \text{ MeV} \quad m_c = 1.5 \text{ GeV}, \\ m_b &= 4.8 \text{ GeV}, \quad |\psi(0)|^2 = \frac{1.642}{4\pi} \text{ GeV}^3. \end{aligned} \quad (14)$$

Here, the B_c wave function at the origin is estimated by using the Buchmueller-Tye potential [42].

The two-loop strong coupling of

$$\frac{\alpha_s(\mu)}{4\pi} = \frac{1}{\beta_0 L} - \frac{\beta_1 \ln L}{\beta_0^3 L^2} \quad (15)$$

is employed in the NLO calculation, in which, $L = \ln(\mu^2/\Lambda_{\text{QCD}}^2)$, $\beta_0 = (11/3)C_A - (4/3)T_F n_f$, $\beta_1 = (34/3)C_A^2 - 4C_F T_F n_f - (20/3)C_A T_F n_f$. Here we take $n_f = 5$ and $\Lambda_{\text{QCD}} = 210 \text{ MeV}$ [43].

In the future, the e^+e^- collider like CEPC or ILC may run at $\sqrt{s} = 250$ GeV or $\sqrt{s} = 500$ GeV. Therefore, we investigate the B_c -pair production with both WWA photon and LBS photon at these two collision energies. Taking the same inputs, we can numerically repeat the LO double pseudoscalar B_c production result in [26]. The full NLO results are presented in Fig.3, Fig.4 and Fig.5. Note, because the cross sections for PV production and VP production are exactly the same, only the PV production results are illustrated.

With $\mu = r\sqrt{m_{B_c}^2 + p_T^2}$, the total cross sections versus r are shown in Fig.3. We observe that, with the NLO corrections, the LO cross sections as well as their dependence on renormalization scale are suppressed. As the \sqrt{s} increased from 250 GeV to 500 GeV, the B_c -pair production rates are enhanced for the WWA photon case but are depressed for the LBS photon case. This may be explained by the different behaviors of WWA and LBS photon, as shown in Fig.1. The WWA photon are more likely to be produced with small momentum fraction x , while the LBS photon tends to be more energetic. Moreover, the partonic cross section $\hat{\sigma}(\gamma + \gamma \rightarrow B_c^+ + B_c^-)$ would decrease with the increase of incident photons center-of-mass energy.

The differential cross sections as functions of p_T , the transverse momentum of one of the two B_c mesons, are shown in Fig.4. It can be seen that as \sqrt{s} increased from 250 GeV to 500 GeV, the WWA distributions are shifted upward slightly, while the LBS distributions are suppressed, especially at the small p_T region. Since the LBS photon are generally more energetic than the WWA photon, the produced B_c pairs may possess larger p_T , which lead to a flatter p_T distribution.

The differential cross sections as functions of Δy , the rapidity difference between the two B_c mesons, are shown in Fig.5. Note, due to $|\Delta y| = 2|y^*|$, the $|\Delta y|$ distribution is equivalent to the $|y^*|$ distribution, where y^* is the rapidity of B_c meson in the photon-photon center-of-mass system. For PP and VV production, the B_c pairs are more likely to be produced around the $y^* = 0$ region. While for the PV or VP production, the peak is located close to $y^* = 0.6$. Since the large energy may lead to large y^* , for the same reason as explained in p_T distribution, the LBS distributions are flatter than the WWA distributions.

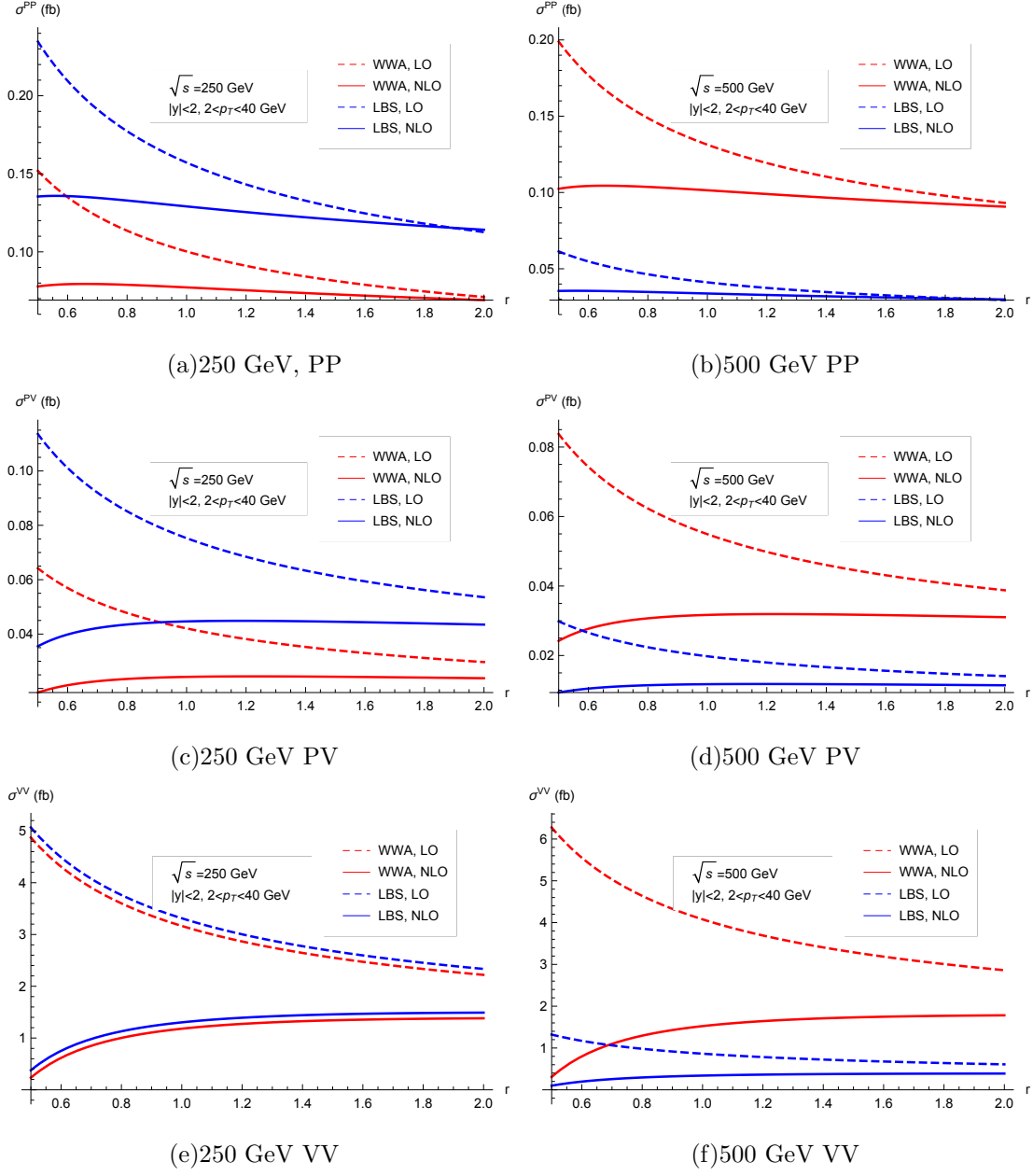


FIG. 3: The LO and NLO cross sections versus r , where $r = \frac{\mu}{\sqrt{m_{B_c}^2 + p_T^2}}$.

In Ref.[30], the productions of B_c pairs in e^+e^- annihilation via virtual γ^* and Z^* are investigated at the NLO QCD accuracy. At large \sqrt{s} , say $\sqrt{s} > 160$ GeV, the cross sections are less than 10^{-6} fb, which are four to six orders of magnitude smaller than the cross sections in our case. It means that at high energy e^+e^- collider, photon-photon

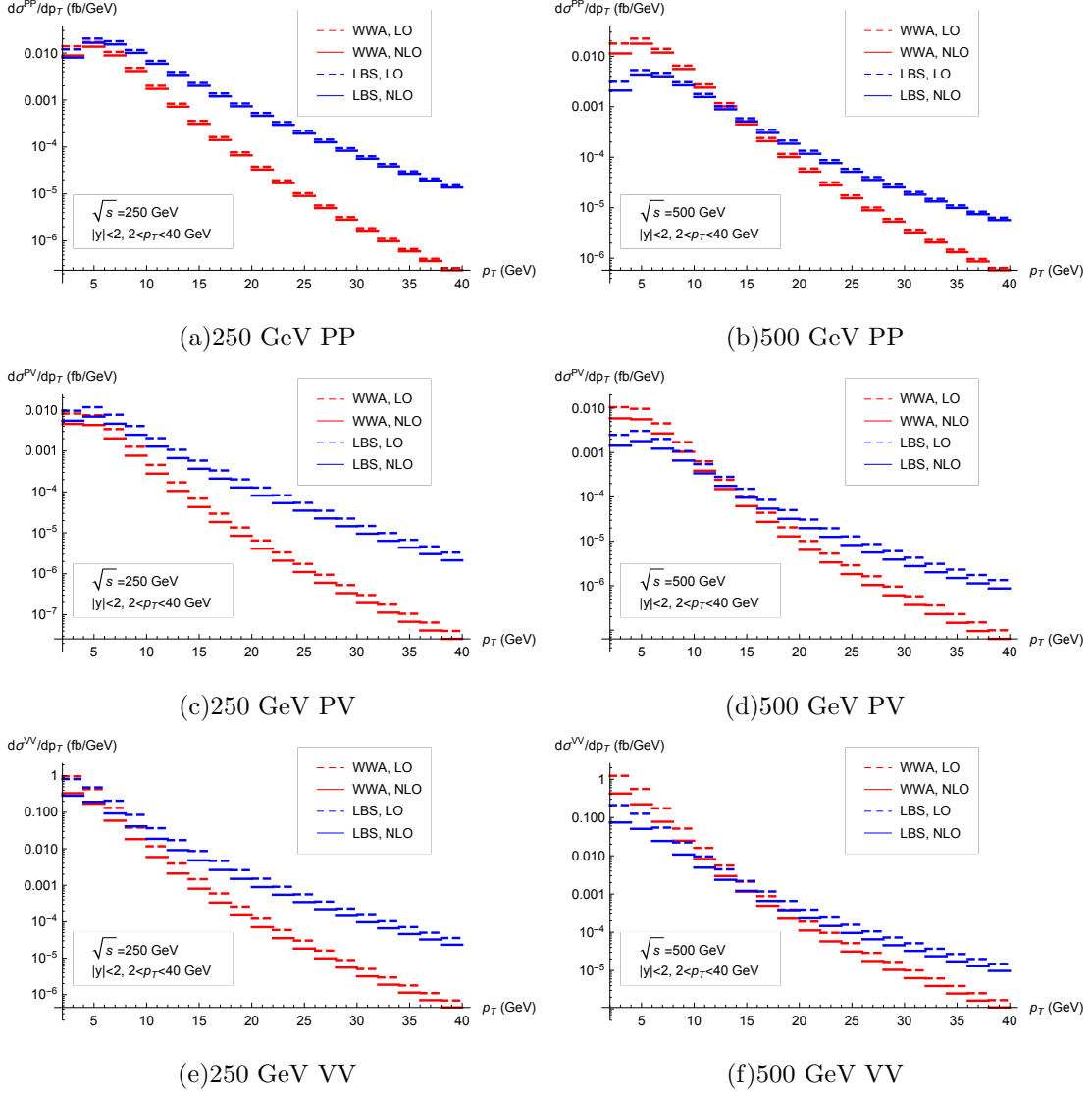


FIG. 4: The LO and NLO differential cross sections versus p_T , the transverse momentum of one of the two B_c mesons. The renormalization scale $\mu = \sqrt{m_{B_c}^2 + p_T^2}$.

collision tends to be the dominant scheme of the B_c -pair production.

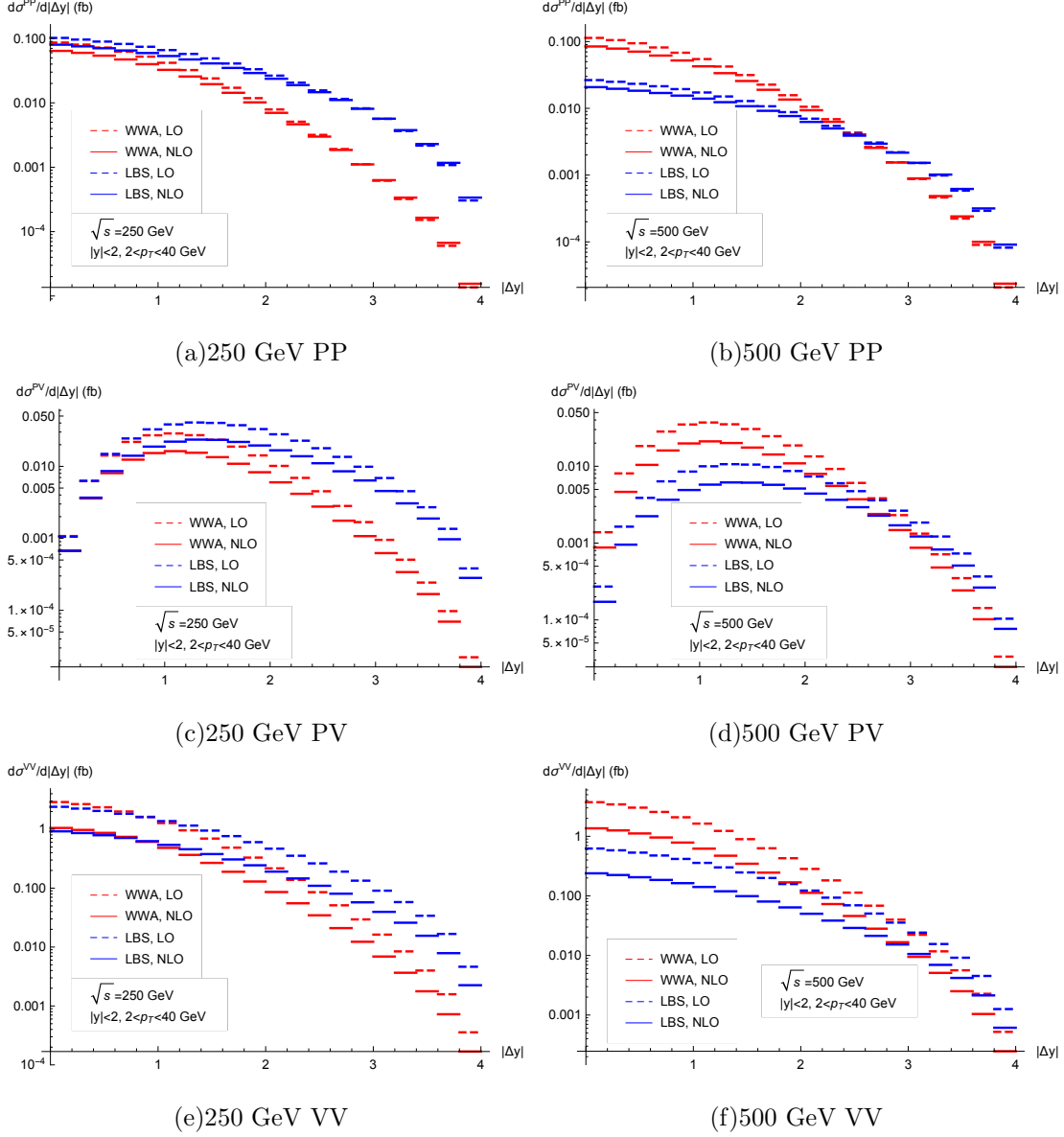


FIG. 5: The LO and NLO differential cross sections versus Δy , the rapidity difference between the two B_c mesons. The renormalization scale $\mu = \sqrt{m_{B_c}^2 + p_T^2}$.

V. SUMMARY

In this work we investigate the B_c -pair production in high energy photon-photon fusion at the NLO accuracy in the NRQCD factorization framework. Various of S -wave B_c states, including configurations of PP, PV, VP and VV, are taken into account. Con-

sidering the leading-order results for B_c -pair production in PV and VP configurations are still missing in the literature, we calculate and provide the analytic results. The total cross section as well as p_T and Δy distributions in e^+e^- collider with $\sqrt{s}=250$ GeV and $\sqrt{s}=500$ GeV are evaluated and presented in figures.

The numerical results show that with the NLO corrections, the LO cross sections are suppressed, and their dependence on renormalization scale are reduced evidently. By comparing with the results in Ref.[30], where the B_c -pair production in e^+e^- annihilation via virtual γ^* and Z^* are investigated, we conclude that at large e^+e^- collision energy, say $\sqrt{s} > 160$ GeV, photon-photon collision will be the dominant source for B_c -pair production.

Last, the NLO calculation of the concerned processes is somewhat time consuming and computer resource exhausting. To fulfill this work, certain technical strategy in the calculation is remarkable, which might be valuable to other relevant calculations.

Acknowledgments

This work was supported in part by the Ministry of Science and Technology of the Peoples' Republic of China(2015CB856703) and by the National Natural Science Foundation of China(NSFC) under the Grants 11975236, 11635009, and 11375200.

-
- [1] F. Abe *et al.* [CDF], Phys. Rev. Lett. **81**, 2432-2437 (1998) [arXiv:hep-ex/9805034 [hep-ex]].
 - [2] F. Abe *et al.* [CDF], Phys. Rev. D **58**, 112004 (1998) [arXiv:hep-ex/9804014 [hep-ex]].
 - [3] G. Aad *et al.* [ATLAS], Phys. Rev. Lett. **113**, no.21, 212004 (2014) [arXiv:1407.1032 [hep-ex]].
 - [4] A. M. Sirunyan *et al.* [CMS], Phys. Rev. Lett. **122**, no.13, 132001 (2019) [arXiv:1902.00571 [hep-ex]].
 - [5] G. T. Bodwin, E. Braaten and G. Lepage, Phys. Rev. D **51**, 1125-1171 (1995); Erratum

- Phys. Rev. D **55**, 5853 (1997) [arXiv:hep-ph/9407339 [hep-ph]].
- [6] C. H. Chang and Y. Q. Chen, Phys. Rev. D **48**, 4086-4091 (1993)
 - [7] C. H. Chang, Y. Q. Chen, G. P. Han and H. T. Jiang, Phys. Lett. B **364**, 78-86 (1995) [arXiv:hep-ph/9408242 [hep-ph]].
 - [8] A. Berezhnoy, A. Likhoded and O. Yushchenko, Phys. Atom. Nucl. **59**, 709-713 (1996) [arXiv:hep-ph/9504302 [hep-ph]].
 - [9] K. Kolodziej, A. Leike and R. Ruckl, Phys. Lett. B **355**, 337-344 (1995) [arXiv:hep-ph/9505298 [hep-ph]].
 - [10] Z. Yang, X. G. Wu and X. Y. Wang, Comput. Phys. Commun. **184**, 2848-2855 (2013) [arXiv:1305.4828 [hep-ph]].
 - [11] X. C. Zheng, C. H. Chang, T. F. Feng and Z. Pan, Sci. China Phys. Mech. Astron. **61**, no.3, 031012 (2018) [arXiv:1701.04561 [hep-ph]].
 - [12] A. Berezhnoy, A. Likhoded and M. Shevlyagin, Phys. Lett. B **342**, 351-355 (1995) [arXiv:hep-ph/9408287 [hep-ph]].
 - [13] K. Kolodziej, A. Leike and R. Ruckl, Phys. Lett. B **348**, 219-225 (1995) [arXiv:hep-ph/9412249 [hep-ph]].
 - [14] A. Berezhnoy, V. Kiselev and A. Likhoded, Phys. Atom. Nucl. **61**, 252-259 (1998) [arXiv:hep-ph/9710429 [hep-ph]].
 - [15] H. Y. Bi, R. Y. Zhang, H. Y. Han, Y. Jiang and X. G. Wu, Phys. Rev. D **95**, no.3, 034019 (2017) [arXiv:1612.07990 [hep-ph]].
 - [16] C. F. Qiao, C. S. Li and K. T. Chao, Phys. Rev. D **54**, 5606-5610 (1996) [arXiv:hep-ph/9603275 [hep-ph]].
 - [17] P. Sun, L. P. Sun and C. F. Qiao, Phys. Rev. D **81**, 114035 (2010) [arXiv:1003.5360 [hep-ph]].
 - [18] C. H. Chang and Y. Q. Chen, Phys. Rev. D **46**, 3845 (1992); Erratum Phys. Rev. D **50**, 6013 (1994).
 - [19] V. Kiselev, A. Likhoded and M. Shevlyagin, Phys. Atom. Nucl. **57**, 689-699 (1994) [arXiv:hep-ph/9401348 [hep-ph]].

- [20] C. F. Qiao, L. P. Sun and R. L. Zhu, JHEP **08**, 131 (2011) [arXiv:1104.5587 [hep-ph]].
- [21] J. Jiang, L. B. Chen and C. F. Qiao, Phys. Rev. D **91**, no.3, 034033 (2015) [arXiv:1501.00338 [hep-ph]].
- [22] C. F. Qiao, L. P. Sun, D. S. Yang and R. L. Zhu, Eur. Phys. J. C **71**, 1766 (2011) [arXiv:1103.1106 [hep-ph]].
- [23] X. C. Zheng, C. H. Chang, X. G. Wu, J. Zeng and X. D. Huang, Phys. Rev. D **101**, no.3, 034029 (2020) [arXiv:1911.12531 [hep-ph]].
- [24] Z. Q. Chen, H. Yang and C. F. Qiao, Phys. Rev. D **101**, no.3, 036009 (2020) [arXiv:1912.02140 [hep-ph]].
- [25] J. Jiang and C. F. Qiao, Phys. Rev. D **93**, no.5, 054031 (2016) [arXiv:1512.01327 [hep-ph]].
- [26] S. Baranov, Phys. Rev. D **55**, 2756-2759 (1997)
- [27] R. Li, Y. J. Zhang and K. T. Chao, Phys. Rev. D **80**, 014020 (2009) [arXiv:0903.2250 [hep-ph]].
- [28] V. Kiselev, Int. J. Mod. Phys. A **10**, 465-476 (1995)
- [29] A. Karyasov, A. Martynenko and F. Martynenko, Nucl. Phys. B **911**, 36-51 (2016) [arXiv:1604.07633 [hep-ph]].
- [30] A. Berezhnoy, A. Likhoded, A. Onishchenko and S. Poslavsky, Nucl. Phys. B **915**, 224-242 (2017) [arXiv:1610.00354 [hep-ph]].
- [31] S. Frixione, M. L. Mangano, P. Nason and G. Ridolfi, Phys. Lett. B **319**, 339-345 (1993) [arXiv:hep-ph/9310350 [hep-ph]].
- [32] I. Ginzburg, G. Kotkin, V. Serbo and V. I. Telnov, Nucl. Instrum. Meth. **205**, 47-68 (1983)
- [33] V. I. Telnov, Nucl. Instrum. Meth. A **294**, 72-92 (1990)
- [34] T. Hahn, Comput. Phys. Commun. **140**, 418-431 (2001) [arXiv:hep-ph/0012260 [hep-ph]].
- [35] R. Mertig, M. Bohm and A. Denner, Comput. Phys. Commun. **64**, 345-359 (1991)
- [36] V. Shtabovenko, R. Mertig and F. Orellana, Comput. Phys. Commun. **207**, 432-444

- (2016) [arXiv:1601.01167 [hep-ph]].
- [37] J. Vermaseren, Nucl. Phys. B Proc. Suppl. **183**, 19-24 (2008) [arXiv:0806.4080 [hep-ph]].
- [38] J. Kuipers, T. Ueda, J. Vermaseren and J. Vollinga, Comput. Phys. Commun. **184**, 1453-1467 (2013) [arXiv:1203.6543 [cs.SC]].
- [39] A. Smirnov, JHEP **10**, 107 (2008) [arXiv:0807.3243 [hep-ph]].
- [40] A. V. Smirnov, Comput. Phys. Commun. **189**, 182-191 (2015) [arXiv:1408.2372 [hep-ph]].
- [41] T. Hahn and M. Perez-Victoria, Comput. Phys. Commun. **118**, 153-165 (1999) [arXiv:hep-ph/9807565 [hep-ph]].
- [42] E. J. Eichten and C. Quigg, Phys. Rev. D **49**, 5845-5856 (1994) [arXiv:hep-ph/9402210 [hep-ph]].
- [43] M. Tanabashi *et al.* [Particle Data Group], Phys. Rev. D **98**, no.3, 030001 (2018)

Appendix

For PP, PV (or VP) and VV production, there are 4, 12 and 36 helicity amplitudes respectively, whereas, half of them are zero. The nonzero helicity amplitudes are

$$\begin{aligned}
& \mathcal{M}_{\text{PP}}^{11}, \mathcal{M}_{\text{PP}}^{44}, \mathcal{M}_{\text{PV,VP}}^{11}, \mathcal{M}_{\text{PV,VP}}^{12}, \mathcal{M}_{\text{PV,VP}}^{13}, \mathcal{M}_{\text{PV,VP}}^{21}, \mathcal{M}_{\text{PV,VP}}^{23}, \mathcal{M}_{\text{PV,VP}}^{22}; \\
& \mathcal{M}_{\text{VV}}^{1111}, \mathcal{M}_{\text{VV}}^{1122}, \mathcal{M}_{\text{VV}}^{1123}, \mathcal{M}_{\text{VV}}^{1132}, \mathcal{M}_{\text{VV}}^{1133}, \mathcal{M}_{\text{VV}}^{1212}, \mathcal{M}_{\text{VV}}^{1213}, \mathcal{M}_{\text{VV}}^{1221}, \mathcal{M}_{\text{VV}}^{1231}, \\
& \mathcal{M}_{\text{VV}}^{2112}, \mathcal{M}_{\text{VV}}^{2113}, \mathcal{M}_{\text{VV}}^{2121}, \mathcal{M}_{\text{VV}}^{2131}, \mathcal{M}_{\text{VV}}^{2211}, \mathcal{M}_{\text{VV}}^{2222}, \mathcal{M}_{\text{VV}}^{2223}, \mathcal{M}_{\text{VV}}^{2232}, \mathcal{M}_{\text{VV}}^{2233}. \quad (16)
\end{aligned}$$

The processes of PV and VP productions are correlated in charge-conjugation transformation, their cross sections should be exactly the same. According convention (10) and (11), the amplitudes satisfy

$$\mathcal{M}_{\text{PV}}^{ijk} = \pm \mathcal{M}_{\text{VP}}^{ijk}, \quad (17)$$

where the plus sign corresponds to $\{i, j, k\} = \{1, 1, 1\}$ and $\{2, 2, 1\}$, the minus sign corresponds to other cases. In addition, the helicity amplitudes satisfy also

$$\mathcal{M}_{\text{PV}}^{122} = \mathcal{M}_{\text{PV}}^{212}|_{k_z \rightarrow -k_z}, \quad \mathcal{M}_{\text{PV}}^{123} = -\mathcal{M}_{\text{PV}}^{213}|_{k_z \rightarrow -k_z};$$

$$\begin{aligned}
\mathcal{M}_{\text{VP}}^{122} &= \mathcal{M}_{\text{VP}}^{212}|_{k_z \rightarrow -k_z}, \quad \mathcal{M}_{\text{VP}}^{123} = -\mathcal{M}_{\text{VP}}^{213}|_{k_z \rightarrow -k_z}; \\
\mathcal{M}_{\text{VV}}^{1123} &= -\mathcal{M}_{\text{VV}}^{1132}, \quad \mathcal{M}_{\text{VV}}^{2223} = -\mathcal{M}_{\text{VV}}^{2232}, \\
\mathcal{M}_{\text{VV}}^{1212} &= -\mathcal{M}_{\text{VV}}^{1221}|_{k_z \rightarrow -k_z} = -\mathcal{M}_{\text{VV}}^{2112}|_{k_z \rightarrow -k_z} = \mathcal{M}_{\text{VV}}^{2121}, \\
\mathcal{M}_{\text{VV}}^{1213} &= -\mathcal{M}_{\text{VV}}^{1231}|_{k_z \rightarrow -k_z} = \mathcal{M}_{\text{VV}}^{2113}|_{k_z \rightarrow -k_z} = -\mathcal{M}_{\text{VV}}^{2131}.
\end{aligned} \tag{18}$$

The analytical expressions for helicity amplitudes can be classified in photon-quark coupling, as

$$\mathcal{M} = \frac{8C_A C_F m_{B_c}^3 \pi^2 \alpha \alpha_s}{3E_1^2 m_b^2 m_c^2} \left[e_c^2 f_1 - e_c e_b (f_2 + f_3) + e_b^2 f_4 + \sum_{i=u,d,s} e_i^2 f_5 \right], \tag{19}$$

where e_q represents the electric charge number of quark q , i.e. $e_c = e_u = \frac{2}{3}$, $e_d = e_s = e_b = -\frac{1}{3}$. The coefficients f_1 and f_4 , f_2 and f_3 are related as per $m_c \leftrightarrow m_b$ exchange:

$$\begin{aligned}
f_{\text{PP},1}|_{m_c \leftrightarrow m_b} &= f_{\text{PP},4}, \quad f_{\text{PP},2}|_{m_c \leftrightarrow m_b} = f_{\text{PP},3}; \\
f_{\text{PV},1}|_{m_c \leftrightarrow m_b} &= -f_{\text{PV},4}, \quad f_{\text{PV},2}|_{m_c \leftrightarrow m_b} = -f_{\text{PV},3}; \\
f_{\text{VP},1}|_{m_c \leftrightarrow m_b} &= -f_{\text{VP},4}, \quad f_{\text{VP},2}|_{m_c \leftrightarrow m_b} = -f_{\text{VP},3}; \\
f_{\text{VV},1}|_{m_c \leftrightarrow m_b} &= f_{\text{VV},4}, \quad f_{\text{VV},2}|_{m_c \leftrightarrow m_b} = f_{\text{VV},3}.
\end{aligned} \tag{20}$$

For the tree amplitudes, f_5 is zero. The analytical results for other coefficients are

$$\begin{aligned}
f_{\text{PP},4}^{11} &= -\frac{r^2(1-r_z^2)}{r-1} - \frac{r_y^2}{(r-1)(1-r_z^2)} + \frac{r(rr_y^2-2r+3)}{r-1} - \frac{2r_y^2}{(1-r_z^2)^2}, \\
f_{\text{PP},3}^{11} &= 1 - \frac{2r_y^2}{(1-r_z^2)^2}, \\
f_{\text{PP},4}^{22} &= -\frac{2r_y^2(2r^2r_y^2-4r^2+4r-1)}{(1-r_z^2)^2} - \frac{r^2(1-r_z^2)}{r-1} + \frac{r_y^2(4r^3-2r^2r_y^2-6r+1)}{(r-1)(1-r_z^2)} + \frac{r(3rr_y^2-2r+3)}{r-1}, \\
f_{\text{PP},3}^{22} &= \frac{2(2r^2-2r-1)r_y^2}{1-r_z^2} - \frac{2r_y^2(2r^2r_y^2-4r^2-2rr_y^2+4r-1)}{(1-r_z^2)^2} + 1; \\
f_{\text{PV},4}^{111} &= ir_m r_y r_z \left(\frac{r}{(r-1)(1-r_z^2)} + \frac{2}{(1-r_z^2)^2} \right), \\
f_{\text{PV},3}^{111} &= -\frac{i2r_m r_y r_z}{(1-r_z^2)^2}, \\
f_{\text{PV},4}^{122} &= \frac{ir_m r_y}{\sqrt{r_y^2+r_z^2}} \left(\frac{2r^2+rr_y^2-3r+2}{(r-1)(1-r_z^2)} + \frac{2(rr_y^2+rr_z-r+1)}{(1-r_z^2)^2} - \frac{r}{r-1} \right), \\
f_{\text{PV},3}^{122} &= \frac{ir_m r_y}{\sqrt{r_y^2+r_z^2}} \left(\frac{2(rr_y^2+rr_z-r-r_y^2-r_z)}{(1-r_z^2)^2} + \frac{2r}{1-r_z^2} \right),
\end{aligned}$$

$$\begin{aligned}
f_{PV,4}^{123} &= \frac{i}{\sqrt{r_y^2+r_z^2}} \left(-\frac{r_y^2(2r-r_y^2-3)}{(r-1)(1-r_z^2)} + \frac{2r_y^2(rr_y^2+2rr_z-r_z)}{(1-r_z^2)^2} - \frac{r(2r_y^2+1)}{r-1} + \frac{r(1-r_z^2)}{r-1} \right), \\
f_{PV,3}^{123} &= \frac{i}{\sqrt{r_y^2+r_z^2}} \left(\frac{2(rr_y^2+2rr_z-r_y^2-r_z)}{(1-r_z^2)^2} - \frac{2(r-1)}{1-r_z^2} \right), \\
f_{PV,4}^{221} &= ir_m r_y r_z \left(\frac{2(2r-1)}{(1-r_z^2)^2} - \frac{r}{(r-1)(1-r_z^2)} \right), \\
f_{PV,3}^{221} &= i2r_m r_y r_z \frac{-1+2r}{(1-r_z^2)^2}; \\
f_{VV,4}^{1111} &= \frac{r^2(1-r_z^2)}{r-1} - \frac{2r-r_y^2-2}{(r-1)(1-r_z^2)} - \frac{r(rr_y^2+1)}{r-1} + \frac{2r_y^2}{(1-r_z^2)^2}, \\
f_{VV,3}^{1111} &= -\frac{2r_y^2}{(1-r_z^2)^2} + \frac{2}{1-r_z^2} - 1, \\
f_{VV,4}^{1122} &= \frac{1}{r_y^2+r_z^2} \left(-\frac{r_y^4+r^2r_y^2+rr_y^2+3r+r_y^2-2}{r-1} - \frac{r^2(1-r_z^2)^2}{r-1} + \frac{r(1-r_z^2)(2rr_y^2+r+1)}{r-1} \right. \\
&\quad \left. + \frac{(r_y^2+1)(2r+r_y^2-2)}{(r-1)(1-r_z^2)} + \frac{2(r_y-1)(r_y+1)r_y^2}{(1-r_z^2)^2} \right), \\
f_{VV,3}^{1122} &= \frac{1}{r_y^2+r_z^2} \left(-\frac{2r_y^2}{(1-r_z^2)^2} + \frac{2(2r_y^2+1)}{1-r_z^2} - r_y^2 - r_z^2 - 2 \right), \\
f_{VV,4}^{1123} &= \frac{r_m r_y r_z}{r_y^2+r_z^2} \left(\frac{r(r_y^2+1)}{(r-1)(1-r_z^2)} - \frac{r}{r-1} + \frac{2(r_y-1)(r_y+1)}{(1-r_z^2)^2} \right), \\
f_{VV,3}^{1123} &= \frac{r_m r_y r_z}{r_y^2+r_z^2} \left(\frac{2}{1-r_z^2} - \frac{2}{(1-r_z^2)^2} \right), \\
f_{VV,4}^{1133} &= \frac{1}{r_y^2+r_z^2} \left(-\frac{r_y^4+3r^2r_y^2+2r^2-rr_y^2-r+r_y^2}{r-1} - \frac{r^2(1-r_z^2)^2}{r-1} + \frac{(r_y^2+1)r_y^2}{(r-1)(1-r_z^2)} \right. \\
&\quad \left. + \frac{r(1-r_z^2)(2rr_y^2+3r-1)}{r-1} + \frac{2(r_y-1)(r_y+1)r_y^2}{(1-r_z^2)^2} \right), \\
f_{VV,3}^{1133} &= \frac{1}{r_y^2+r_z^2} \left(\frac{2r_y^2}{1-r_z^2} - \frac{2r_y^2}{(1-r_z^2)^2} - r_y^2 - r_z^2 \right), \\
f_{VV,4}^{1212} &= \frac{r_m^2}{\sqrt{r_y^2+r_z^2}} \left(-\frac{r(r_y^2+1)}{(r-1)(1-r_z^2)} - \frac{2(rr_y^2+r_z)}{(1-r_z^2)^2} + \frac{r}{r-1} \right), \\
f_{VV,3}^{1212} &= \frac{r_m^2}{\sqrt{r_y^2+r_z^2}} \left(-\frac{2(rr_y^2-r_y^2-1)}{(1-r_z^2)^2} - \frac{2}{1-r_z^2} \right), \\
f_{VV,4}^{1213} &= \frac{r_m r_y}{\sqrt{r_y^2+r_z^2}} \left(\frac{r(2r-r_y^2-3)}{(r-1)(1-r_z^2)} - \frac{2(rr_y^2+rr_z+r-1)}{(1-r_z^2)^2} + \frac{r}{r-1} \right), \\
f_{VV,3}^{1213} &= \frac{r_m r_y}{\sqrt{r_y^2+r_z^2}} \left(\frac{2(r-1)}{1-r_z^2} - \frac{2(rr_y^2+rr_z+r-r_y^2-1)}{(1-r_z^2)^2} \right), \\
f_{VV,4}^{2211} &= \frac{2r_y^2(2r^2r_y^2-1)}{(1-r_z^2)^2} + \frac{r^2(1-r_z^2)}{r-1} - \frac{4r^3r_y^2-2r^2r_y^4-4r^2r_y^2-2rr_y^2-2r+r_y^2+2}{(r-1)(1-r_z^2)} - \frac{r(3rr_y^2+1)}{r-1}, \\
f_{VV,3}^{2211} &= \frac{2r_y^2(2r^2r_y^2-2rr_y^2-1)}{(1-r_z^2)^2} - \frac{2(2r^2r_y^2-2rr_y^2-r_y^2-1)}{1-r_z^2} - 1, \\
f_{VV,4}^{2222} &= \frac{1}{r_y^2+r_z^2} \left(\frac{2r_y^2(2r^2r_y^4+2r^2r_y^2-r_y^2+1)}{(1-r_z^2)^2} - \frac{r^2(1-r_z^2)^2}{r-1} + \frac{4r^3r_y^2-5r^2r_y^4-7r^2r_y^2-3rr_y^2+r+r_y^2-2}{r-1} \right. \\
&\quad \left. - \frac{8r^3r_y^4+4r^3r_y^2-2r^2r_y^6-10r^2r_y^4-4r^2r_y^2-2rr_y^4+2r+r_y^4-r_y^2-2}{(r-1)(1-r_z^2)} + \frac{r(1-r_z^2)(4rr_y^2+r+1)}{r-1} \right), \\
f_{VV,3}^{2222} &= \frac{1}{r_y^2+r_z^2} \left(\frac{2r_y^2(2r^2r_y^4+2r^2r_y^2-2rr_y^4-2rr_y^2-2r_y^2-1)}{(1-r_z^2)^2} - \frac{2(4r^2r_y^4+2r^2r_y^2-4rr_y^4-2rr_y^2-r_y^4-3r_y^2-1)}{1-r_z^2} \right)
\end{aligned}$$

$$\begin{aligned}
& 4r^2r_y^2 + -4rr_y^2 - 3r_y^2 - r_z^2 - 2), \\
f_{VV,4}^{2223} &= \frac{r_m r_y r_z}{r_y^2 + r_z^2} \left(\frac{r(4r - r_y^2 - 5)}{(r-1)(1-r_z^2)} - \frac{2(2rr_y^2 + 2r + r_y^2 - 1)}{(1-r_z^2)^2} + \frac{r}{r-1} \right), \\
f_{VV,3}^{2223} &= \frac{r_m r_y r_z}{\sqrt{r_y^2 + r_z^2}} \left(\frac{2(2r-1)}{1-r_z^2} - \frac{2(2rr_y^2 + 2r + r_y^2 r_z - r_y^2 - 1)}{(1-r_z^2)^2} \right), \\
f_{VV,4}^{2233} &= \frac{1}{r_y^2 + r_z^2} \left(\frac{2r_y^2(2r^2r_y^4 + 6r^2r_y^2 + 4r^2 - 4rr_y^2 - 4r - r_y^2 + 1)}{(1-r_z^2)^2} - \frac{r^2(1-r_z^2)^2}{r-1} + \frac{r(1-r_z^2)(4rr_y^2 + 3r - 1)}{r-1} \right. \\
&\quad \left. - \frac{r_y^2(8r^3r_y^2 + 12r^3 - 2r^2r_y^4 - 14r^2r_y^2 - 24r^2 + 2rr_y^2 + 10r + r_y^2 + 1)}{(r-1)(1-r_z^2)} + \frac{4r^3r_y^2 - 5r^2r_y^4 - 13r^2r_y^2 - 2r^2 + 3rr_y^2 + r + r_y^2}{r-1} \right), \\
f_{VV,3}^{2233} &= \frac{1}{r_y^2 + r_z^2} \left(- \frac{2r_y^2(4r^2r_y^2 + 6r^2 - 4rr_y^2 - 6r - r_y^2)}{1-r_z^2} + \frac{2r_y^2(2r^2r_y^4 + 6r^2r_y^2 + 4r^2 - 2rr_y^4 - 6rr_y^2 - 4r + 1)}{(1-r_z^2)^2} \right. \\
&\quad \left. + 4r^2r_y^2 - 4rr_y^2 - 3r_y^2 - r_z^2 \right). \tag{21}
\end{aligned}$$

Here, $r = m_b/(m_b + m_c)$. The analytical results for the one-loop amplitude are lengthy, and are presented in the supplementary files attached to the arXiv preprint.